Measurement 216 (2023) 112889

Contents lists available at ScienceDirect

Measurement

journal homepage: www.elsevier.com/locate/measurement

XPQRS: Expert power quality recognition system for sensitive load applications

Muhammad Umar Khan [a,b,1], Sumair Aziz [a,b,*,1], Adil Usman [b]

[a] Human-Centred Technology Research Centre, Faculty of Science and Technology, University of Canberra, Canberra, ACT 2617, Australia
[b] Department of Electronics Engineering, University of Engineering and Technology Taxila, Taxila, 47040, Pakistan

ARTICLE INFO

Keywords:
Approximated derivatives
Feature extraction
Power quality disturbances
Single power cycle
Support vector machine

ABSTRACT

Power Quality (PQ) disturbances of a few milliseconds duration may lead to malfunctioning the sensitive devices connected to the network. This necessitates detecting these PQ disturbances in a minimum time before affecting the sensitive load and adopting countermeasures. An expert PQ recognition system (XPQRS) is proposed to identify seventeen types of PQ events using only one power cycle acquired at 5 kHz. In XPQRS, the input PQ signal is first concatenated with its four derivatives to highlight the deviations. Log energy, Shannon energy, and mobility parameters, extracted from the resultant vectors, are then fed to Quadratic Support Vector Machine. XPQRS offers 96.5% accuracy and provides fast decisions in 34.99 ms which makes it suitable for its implementation on an embedded system. XPQRS shows noise immunity and outperforms the previous studies in terms of decision time, accuracy, and computational complexity.

1. Introduction

Today, the proliferation of power electronic devices, nonlinear loads, and highly penetrated distributed energy resources in electric power networks has caused growing concerns for power quality (PQ) issues from both utilities and customers. The voltage sag, swell, and interruptions are caused by lines to ground, unbalanced, or nonlinear load. Power electric converters and arc furnaces may lead to flickers and fluctuations. The usage of adjustable-speed drives and energy-efficient equipment may trigger the harmonics. Spikes or transients can be observed while switching off large loads or capacitor banks for transformer energizing and power factor improvement. The integration of renewable energy has introduced the problem of time-varying harmonics being generated alongside frequency deviations [1]. International standards, such as IEC 61000, IEEE 1159, and EN 50160 define a set of rules for the PQ limits [2,3]. PQ disturbances beyond these limits can cause failure or mal-operation of sensitive electrical and electronic devices, damage to computer-based systems, and malfunction or permanent loss of PLC controls protection, and relaying apparatus in the industry [4–6]. Moreover, for manufacturers with automated production lines, a few cycles of interruption, voltage sag, voltage swell, or short circuit can affect the entire production line and result in a significant loss in the process industry [7]. For example, a typical semiconductor foundry in Taiwan loses $100,000 to $1,000,000 per sag event [4]. Such sensitive industrial equipment can be protected from these hazardous variations if they are recognized accurately in the minimum possible time. Accurate detection and recognition with fast processing can significantly enhance the efficiency of a controller used for the mitigation of power quality disturbance (PQD).

Various PQD detection and classification techniques have been presented by different researchers. A power disturbance event recognition technique using Wavelet Packet Transform (WPT) and Support Vector Machines (SVM) presented 98.3% accuracy in classifying 8 types of PQDs. The disturbance signals of 12 cycles were acquired at a 12.5 kHz sampling rate and were recognized using an SVM classifier [8]. Empirical mode decomposition (EMD) with Artificial Neural Network (ANN) showed 100% accuracy with 9 disturbance classes. A PQD signal length of 10 cycles was used with a 20.48 kHz sampling frequency [9]. Compressed Sensing (CS) and Deep Convolution Neural Networks (DCNN) classified 15 PQD events of 10 cycles duration with greater than 99% accuracy [10]. Stockwell Transform (SWT) technique combined with neural network (NN) offered an average accuracy of 94.7% in recognizing ten disturbance classes. 10 cycles were used for the analysis of signals which were acquired at a sampling rate of 200 kHz [11].

S-Transform (ST) based scheme exhibited an average accuracy of up to 99% in identifying 15 PQD classes under various noisy conditions.

* Corresponding author at: Human-Centred Technology Research Centre, Faculty of Science and Technology, University of Canberra, Canberra, ACT 2617, Australia.
E-mail addresses: umar.khan@canberra.edu.au (M.U. Khan), sumair.aziz@canberra.edu.au (S. Aziz), adil.usman@uettaxila.edu.pk (A. Usman).
[1] These authors contributed equally to this work.

https://doi.org/10.1016/j.measurement.2023.112889
Received 9 January 2023; Received in revised form 8 April 2023; Accepted 12 April 2023
Available online 28 April 2023

The disturbance signal length of 10 cycles was used with a sampling frequency of 6.4 kHz [12]. Modified S-Transform (MST) detected 8 types of PQD signals with different noise levels and showed an accuracy of up to 100%. Here again, 10 cycles of signals obtained at a 15.36 kHz sampling rate were involved to attain the reported results [13]. In a technique, SVM with cubic kernel classified 8 classes using 10 cycles of the signal [14]. A monitoring system for source voltage distortion used higher-order statistics (HoS) to extract features and Neuro Tree (NT) to detect 20 disturbances, which demonstrated 97% accuracy [15]. The detection method using Flexible Entropy based Feature Selection (FEFS) and multi-class SVM (MC-SVM) presented maximum accuracy of 98.65% in classifying 9 PQDs with 20 cycles of PQD signal [16].

Discrete Wavelet Transform (DWT) based disturbance detection techniques have also been proposed in the literature. In one such study, the histogram and Discrete Wavelet Transform (DWT) method for feature extraction. Extreme Learning Machine (ELM) classification was employed which showed 100% accuracy of disturbance detection using this large number of 10 cycles of a signal obtained using a sampling frequency of 10 kHz. Only six classes were recognized using this technique [17]. Another ELM-based power system disturbance recognition algorithm was presented. Particle Swarm Optimization (PSO) was employed in this study for parameters determination and feature selection of ELM. 97.6% accuracy was claimed with 10 cycles of the signal used for disturbance detection applying a 12.8 kHz sampling frequency. Ten types of PQD events were classified using the presented method [18]. Although the DWT-based disturbance detection methods present good accuracy but the long computation time is the main drawback of these algorithms. However, the combination of the DWT feature extraction method and the One-Class SVM (OCSVM) classifier for disturbance detection of only five classes showed an accuracy of 93%. 10 cycles of disturbance signal were processed in this method but accuracy is still very low [19]. A recently presented DWT and Correlation Coefficients based detection and classification method showed an average accuracy rate of 98.17% against 9 events. But this accuracy was obtained with a long window size of 15 cycles and a high sampling rate of 20 kHz [20].

A combination of improved Principal Component Analysis (IPCA) and 1-Dimensional Convolution Neural Network (1D-CNN) for PQ detection showed a maximum of 99.92% accuracy against 12 PQD classes. 10 cycles window of the PQD signal with a sampling frequency of 10 kHz was used to deliver the reported performance. While implementing this algorithm on a real-time PQ monitoring system, the computational cost with a large number of cycles and high sampling frequency would be very high [21]. Fusion of Time Domain Descriptor (FTDD) based feature extraction method extracted distinguished features. Its performance under various noisy conditions was analyzed by feeding 10 cycles voltage signal obtained using a 10 kHz sampling frequency to Multiclass-SVM (M-SVM) and as well as Naïves Bayes (NB) classifiers. The maximum mean accuracy attained with both M-SVM and NB is above 99%. It is worth mentioning that only the computation of features takes 1.57 s which shows its high computation cost. Moreover, the algorithm classified only 6 PQD events [22].

It is noteworthy that most of the techniques in the scientific literature related to PQD detection and classification using voltage signals of 10 cycles or more acquired at the rate of 10 kHz sampling rate to train and test the algorithm. A long signal length of 10 cycles or more and a high sampling frequency of 10 kHz or greater results in a high computational burden/cost. In order to implement a PQD recognition algorithm in a real system, it is desirable that the algorithm should be computationally efficient and presents the minimum possible processing time. However, the use of a large number of cycles and a high sampling rate, for delivering detection and classification decision make these algorithms computationally complex and hence make them misfit for their use in real-world protection circuits.

There are a few studies related to PQD detection and classification, in which a sampling rate of less than 10 kHz is used for voltage signal acquisition. A strong tracking filter (STF) was used to extract the relevant features to characterize the PQDs and then ELM was employed to classify 20 disturbance events. A low rate of correct decisions of 92.6% was achieved with 10 cycles window of signals acquired at a 6.4 kHz sampling rate [23]. A combination of the DWT feature extraction technique and hierarchical ELM (H-ELM) classifier identified 15 disturbances with a low accuracy of 95%. A signal length of 10 cycles was used for the processing with a 6.4 kHz sampling frequency [24]. In another reported work, various energy levels were computed using DWT coefficients and Parseval's theorem. These energy levels were used as features. ANN technique was used to detect only 6 power disturbances based on 10 cycles window of voltage signal obtained at a 6.4 kHz sampling rate [25]. In a Stockwell transform and decision-based method, Stockwell transform was developed on the basis of moving, localizing, and scalable Gaussian window to detect PQDs with 15 cycles acquired utilizing 3.2 kHz. The extracted features were fed to Decision Tree (DT) to recognize only nine types of events [26]. A disturbance recognition algorithm, based on Time–Frequency (TF) analysis and DT classifier exhibited 99.9% accuracy against 12 PQD classes. It is important here to mention that this method utilizes a very low sampling frequency of 3.2 kHz but the disturbance detection process requires 50 cycles to classify the events which greatly increases the computational complexity [27]. Similarly, the PQD signal detection method based on Multi-resolution S-Transform (MST) and DT offers greater than 99% accuracy. But again, it uses 50 cycles of the signal acquired at a 3.2 kHz sampling rate to perform its processing. The proposed method recognized 16 PQD events [28]. ST with rule-based DT detection technique used 10 cycles of a signal obtained using 3.2 kHz sampling frequency to demonstrate maximum overall efficiency of 99.4%. This algorithm classified only 7 disturbance classes [29]. The Modified S-Transform (MST) with Parallel Stacked Sparse Auto-Encoder (PSSAE) disturbance detection scheme showed an accuracy of 99.06% in classifying 13 events. 10 cycles of voltage signals were acquired at a low sampling rate of 2.56 kHz [30]. Double-Resolution S-Transform (DRST) was used to extract features and Directed Acyclic Graph Support Vector Machine (DAG-SVMs) was used for PQD detection and classification of 9 PQD classes. The technique was implemented on DSP hardware. It showed 80% accuracy in recognizing the 10 cycles signals acquired at a 5 kHz sampling rate [31]. Variational mode decomposition (VMD) and the Deep Stochastic Configuration Network (DSCN) for power quality (PQ) disturbance detection have maximum mean accuracy of 99.4% against only 7 events. Mean, variance, and kurtosis were extracted from the instantaneous amplitude of the decomposed modes. A window size of 10 cycles was used for signal analysis which was acquired at a 2 kHz sampling rate [32]. Variational Mode Decomposition (VMD) and ST were used for feature extraction and Support Vector Machine (SVM) for classification. An accuracy of 99.66% in classifying 9 PQD events was reported. 10 cycles of voltage signals with 2 kHz sampling frequency were used to train and test the algorithm [33]. Recently presented Space Vector Ellipse in Complex Plane classification technique showed good accuracy with a very low sampling frequency of 2 kHz. But 10 cycles of voltage signal were used for signal analysis. This scheme recognized only 10 classes [34]. In a comparison of the classical Long Short Term Memory (LSTM) Recurrent Neural Network (RNN) classification method, the Convolutional Auto-Encoder compression architecture-based stacked LSTM RNN method showed better performance with respect to classification accuracy and processing time. A 15 cycles window was used to identify the disturbance signals obtained using a 1 kHz sampling frequency. Nine classes were tested for the performance analysis of the algorithm [35]. It can be observed from the above-reviewed studies that, although, they employ low sampling rates but some of them are still using 10 cycles of signals for the analysis due to which, they are not suitable to implement on hardware. Some of them achieved low accuracy of classification due to low signal resolution. In order to increase the accuracy, some researchers increased the number of cycles up to 50 cycles. But they could classify only a few PQD classes with low sampling frequency. Similarly,

with a sampling frequency less than 3.2 kHz, less than or equal to ten PQD events could be recognized while using a high number of cycles of the input voltage signal. In a PQD classification method, colorized continuous wavelet transform coefficients of the voltage signals were applied to convolutional neural networks as an image file. Although 8 cycles were used for signal analysis, only four classes of single events were recognized. Moreover, a 25.6 kHz sampling frequency was used for signal acquisition and processing. Last but not least only 5 PQD classes were recognized using this method [36].

According to research on machine learning methods for PQD detection and classification, the number of samples per cycle will rise if the PQ signal is acquired at a high sampling frequency. As a result, the signal's resolution is raised, but an increase in computational cost follows. In contrast, using a low sampling rate results in few samples that provide a poor resolution of the signal, which may result in the loss of information about it and a reduction in the accuracy of the system. Similarly, employing a large number of cycles of PQD signal may enhance the accuracy of recognition but the computational burden is also increased.

To design an algorithm for the detection and classification of multi-complex PQD events with high accuracy and low computational cost, three points must be considered: (a) the most relevant features which represent the PQD signal should be employed, so that the relevant information can be extracted from a signal with less number of cycles of voltage signals acquired using low sampling frequency. (b) there should be a balance between the signal resolution, number of cycles, and computational complexity while keeping the accuracy high. (c) the classifier used must exhibit maximum accuracy in such constrained conditions. Considering these guidelines, the major contributions of the proposed Expert Power Quality Recognition System (XPQRS) method can be listed:

1. XPQRS is designed to classify PQ disturbances using only one cycle of the input signal that is acquired at a very low sampling frequency of 5 kHz.
2. Derivative-based pre-processing technique is used to magnify the deviations in the input PQ signals.
3. Only three simple features capable of characterizing the seventeen multi-complex PQ disturbance classes are used.
4. High-performance metrics (96.5% accuracy) and fast decision time (34.99 ms) of the proposed classification scheme are the key attributes that show the suitability of the method for its implementation in real protection and PQ disturbance monitoring systems to avoid malfunctioning or damage to the sensitive loads.
5. XPQRS, trained on a dataset containing 100 data points per PQ signal, shows the satisfactory performance when compared to the previous state-of-the-art and even under noisy conditions.

This article is organized as follows: Section 2 provides details of the PQD dataset used in this study. Section 3 corresponds to the methodology of the proposed XPQRS, explaining the step-by-step procedure for the recognition of PQD events. Section 4 presents the results and discussion in relation to other studies. Section 5 concludes this article and gives insights into the future directions.

2. Materials

In this research, seventeen types of multi-complex PQ signals are considered, nine of which are single events and eight are combined disturbances. The group of single events includes normal (pure sine), sag, swell, interruption, transient/spike, oscillatory transient, harmonics, flicker, notch, and combined disturbances are sag with harmonics, swell with harmonics, flicker with sag, flicker with a swell, sag with oscillatory transient, swell with oscillatory transient, harmonics with sag and harmonics with a swell. PQ signal data was generated using mathematical models provided by IEEE Std. 1159 [37]. The fundamental frequency of each signal was 50 Hz. 1000 signals of each PQ disturbance were synthesized using a sampling frequency of 5 kHz. So, there is a total of 17 000 signals in the dataset. It is worth mentioning that each signal consists of only one cycle i.e., 100 data points. An ideal PQ signal (PQ_1) can be defined by the following equation.

$$PQ_1 = A * sin(\omega t - \varphi) \tag{1}$$

The rest of the PQ disturbance classes are described as follows.

2.1. Voltage sag (PQ_2)

The decrease in nominal RMS voltage between 0.1 p.u. and 0.9 p.u. is known as voltage sag. Voltage sag might last anywhere from 0.5 cycles and 1 min. Sag is the most frequent occurrence due to single line-to-ground (SLG) faults, starting large motors, and activities requiring heavy currents. Another way to describe voltage sag is as a temporary drop in voltage level.

$$PQ_2 = A\{1 - \alpha(u(t - t_1) - u(t - t_2))\}sin(\omega t - \varphi) \tag{2}$$

where, $T \leq t_2 - t_1 \leq (N-1)T$ and $0.1 \leq \alpha \leq 0.9$

2.2. Voltage swell (PQ_3)

The increase in nominal RMS voltage between 1.1 p.u. and 1.8 p.u. is known as voltage swell. Unlike sag, voltage swell occurs less frequently. Voltage swell can oscillate from 0.5 cycles to 1 min in duration, just like sag. The factors that could cause a voltage swell include a light load on the system, an erroneous tap setting on the transformer, and more. Voltage swell events can have serious consequences, including device overheating and substantial iron loss in most machine applications.

$$PQ_3 = A\{1 + \beta(u(t - t_1) - u(t - t_2))\}sin(\omega t - \varphi) \tag{3}$$

where, $T \leq t_2 - t_1 \leq (N-1)T$ and $0.1 \leq \beta \leq 0.9$

2.3. Interruption (PQ_4)

The decrease in RMS voltage results in a voltage interruption that is not higher than 0.1 p.u. It is the worst scenario for voltage sag. It results from a loose connection, significant flaws, and the re-closing of an electrical switch. The voltage interruption causes the system as a whole to trip inconveniently and operate incorrectly.

$$PQ_4 = A\{1 - \rho(u(t - t_1) - u(t - t_2))\}sin(\omega t - \varphi) \tag{4}$$

where, $T \leq t_2 - t_1 \leq (N-1)T$ and $0.9 \leq \rho \leq 1$

2.4. Impulsive transient (PQ_5)

The electrical clients encounter impulsive transient, which causes a disturbing disruption. Impulsive transients cause a unidirectional, positive-extreme shift in the size of the voltage magnitude immediately. Short rise and fall times are a defining feature of this occurrence. A lightning strike is a factor that is most often known to cause impulsive transients.

$$PQ_5 = A[sin(\omega t - \varphi) - \psi(e^{(-750(t-t_a))} - e^{-344(t-t_a)})(u(t - t_1) - u(t - t_2))] \tag{5}$$

where, $0.222 \leq \psi \leq 1.11$, $T \leq t_a \leq (N-1)T$, and $t_b = t_a + 1$ ms

2.5. Oscillatory transient (PQ_6)

In addition to the prior PQD events, oscillatory transients may also occur in power lines. A transient is an abrupt shift in voltage level. This uncomfortable influence often lasts between 5 μs and 50 ms. This type of transient can have a maximum magnitude in arise of up to 2.0 p.u. The extreme oscillatory transient is typically between 1.2 and 1.5 p.u. in size. Positive or negative oscillatory transients can cause abrupt variations in the event's magnitude. These were based on chosen frequency ranges that correlate to typical categories of oscillatory transient occurrences in power systems. The oscillation's frequency can be used to identify the source of the disruption. The transient may be caused by the capacitor switching, a load, or the re-closing of a circuit breaker.

$$PQ_6 = A[sin(\omega t - \varphi) + \beta e^{-\frac{(t-t_I)}{\tau}} sin(\omega_n(t-t_I) - \theta)(u(t-t_{II}) - u(t-t_I))] \quad (6)$$

where, $300 \le f_f \le 900$ Hz, $w_n = 2\pi f_n$; 8 ms $\le \tau \le$ 40 ms; $-\pi \le \theta \le \pi$, and $0.05T \le t_{II} - t + I \le \frac{N}{3.33}T$

2.6. Harmonics (PQ_7)

Due to the presence of non-linear loads, harmonics are produced in an electric power system. Harmonics in a system lead to engine torque fluctuations, overheating of conductors, and incorrect activation of factor speed drives. Non-linear loads like computers and printers, fluorescent lamps, battery chargers, and many more cause the most crucial events to happen. A harmonics event is when several frequencies are added to the voltage waveform's power frequency.

$$PQ_7 = A[sin(\omega t - \varphi) + \sum_{n=3}^{7} \alpha_n sin(n\omega t - \theta_n)] \quad (7)$$

2.7. Voltage flicker (PQ_{10})

Voltage flicker is characterized by cyclic variations in voltage magnitude that have an amplitude of less than 10% of the nominal value. Voltage variations do not hurt electrical equipment; instead, they could cause changes to how brightly light sources are produced. Utility customers may complain about voltage flicker because it causes an unpleasant visual sense.

$$PQ_{10} = A[1 + \lambda sin(\omega_f t)]sin(\omega t - \varphi) \quad (8)$$

where $0.05 \le \lambda \le 0.1$, $8 \le f_f \le 25$ Hz and $\omega_f = 2\pi f_f$

2.8. Notch (PQ_{17})

A notch is a situation when there is a brief decline in voltage magnitude towards zero (usually in microseconds). Remember that a transient voltage event differs from a voltage notch. Some transients can also cause the voltage to drop suddenly as it approaches the zero-crossing axis. Voltage notching is a steady-state situation in this case, whereas transients only happen briefly when there is any transitory disturbance to the system. In Silicon Controlled Rectifiers (SCR), commutation produces a voltage notch. Any product with a phase-controlled rectifier in the front-end circuit will result in a voltage notch of some size, e.g., DC drives, regulated rectifiers, SCR-controlled AC heating circuits, light dimmers, etc. The electrical system's natural frequencies can be excited by the notch, which causes the system voltage to exhibit more non-typical harmonics. Due to the frequency harmonics present during notch events, this may potentially cause radio interference and impair the facility's delicate logic and communication systems. Voltage notching can increase operational temperatures and result in additional losses in power factor capacitors.

$$PQ_{17} = A[sin(\omega t - \varphi) - sign(sign(\omega t - \varphi)) \times \sum_{n=0}^{N.c-1} k(u(t - (t_c + sn)) - u(t - (t_d + sn)))] \quad (9)$$

where $0.01T \le t_d - t_c \le 0.05T$,
$t_d \le s; t_c \ge 0$,
$0.1 \le k \le 0.4$; $c = \{1, 2, 4, 6\}$; $s = \frac{T}{c}$.

2.9. Combined PQD events

In addition to PQ consisting of single events, various second-order complex PQ disturbances were considered for analysis. The list of these multi-complex events where various single-event PQ occur at the same time is as follows:

1. Sag with Harmonics (PQ_8)
2. Swell with Harmonics (PQ_9)
3. Flicker with Sag (PQ_{11})
4. Flicker with Swell (PQ_{12})
5. Sag with Oscillatory Transient (PQ_{13})
6. Swell with Oscillatory Transient (PQ_{14})
7. Harmonics with Sag (PQ_{15})
8. Harmonics with Swell (PQ_{16})

Example signals for single-cycle PQ disturbance classes used in this research are presented in Fig. 1.

3. Method

Fig. 2 illustrates the design of this research for the detection and classification of multi-complex power quality disturbances using one cycle of the input voltage signal. The proposed methodology encompasses three major steps; 1. Pre-processing, 2. Feature Extraction, and 3. Classification. In the pre-processing step, the approximated derivatives were obtained by employing the first four derivative operators for the pre-processing of the input voltage signal that magnifies the change upon the occurrence of PQ disturbance. The performance of the recognition algorithm was also evaluated using the original signal and various combinations of derivative-operated signals. In the feature extraction step, three simple features, i.e., Log Energy (LE), Shannon Energy (SE), and Mobility (Mob), were extracted from pre-processed signals as well as from the original PQ signal. In order to compare the characterization capability of the proposed features, some traditional features from various domains (time and spectral) were also included in the experimentation. After rigorous experimentation on a pool of classifiers, the support vector machine with the quadratic kernel (QSVM) was proposed for the designed PQ disturbance recognition system.

3.1. Pre-processing

In this study, differentiation is employed as the pre-processing technique which enhances the change arising due to a PQ disturbance event during a normal voltage signal. Considering X is a vector of input voltage signal having length n, the pre-processing technique computes the differences between the successive elements of the vector.

$$X = [X(1), X(2), X(3), \dots X(n)] \quad (10)$$

where n denotes the number of samples in the acquired PQ signal. If $D^{(1)}$ = approximated derivative of X where the matrix $D^{(1)}$ is the first-order approximated derivative of X, then

$$D^{(1)} = d(X) \quad (11)$$

i.e.

$$D^{(1)} = [X(2) - X(1), X(3) - X(2), \dots, X(n) - X(n-1)] \quad (12)$$

High order derivative of a vector can also be taken. If the derivative of vector X is taken a second time,

$$D^{(2)} = d_2(X) \quad (13)$$

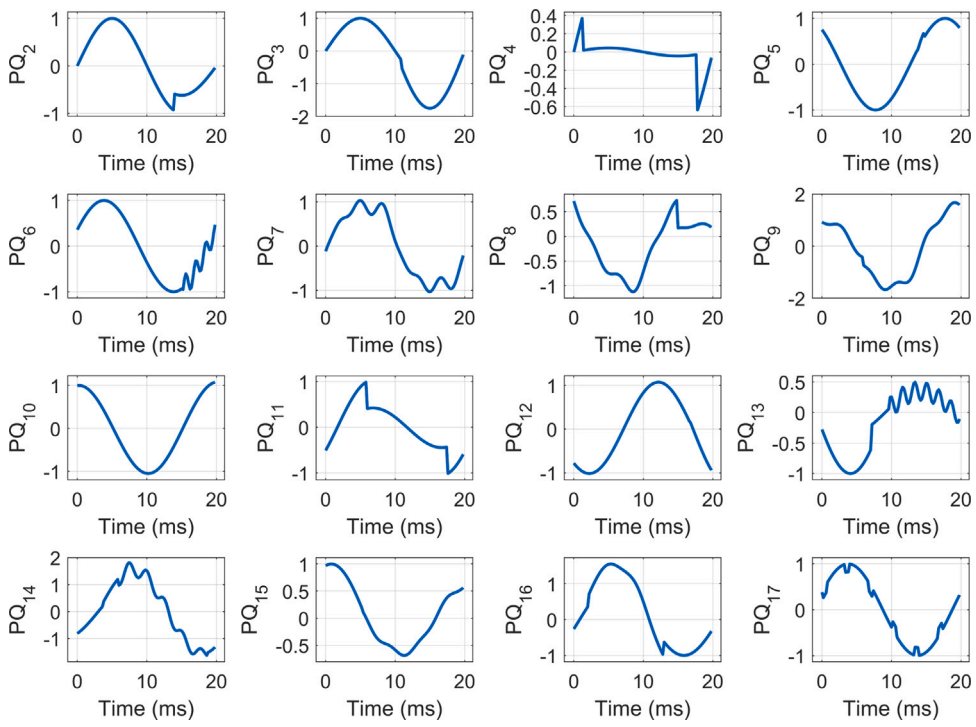

Fig. 1. Example waveforms for single cycle PQ disturbances used in this research.

Let, $X(2)-X(1)=L(1), X(3)-X(2)=L(2), \ldots, X(n)-X(n-1)=L(n-1)$, then Eq. (12) takes the form:

$$D^{(1)}=[L(1), L(2), L(3), \ldots, L(n-1)], \tag{14}$$

Similarly,

$$D^{(2)}=[L(2)-L(1), L(3)-L(2), \ldots, L(n-2)-L(n-1)], \tag{15}$$

$$D^{(3)}=(D^{(2)})^{(1)}, \tag{16}$$

$$D^{(4)}=(D^{(3)})^{(1)} \tag{17}$$

where the dimension of D is n, the $D^{(1)}$ dimension is $n-1$, and the $D^{(2)}$ dimension is $n-2$. The size of the vector decreases with the order of the derivative. In general, the approximated derivative can be represented as:

$$D^{(k)}=(D^{(k-1)})^{(1)} \tag{18}$$

where k is the order of approximated derivative.

For example,

Let, $X=[180, 185, 192, 196, 220]$, i.e., n = 5

$D^{(1)}=[(185-180), (192-185), (196-192), (220-196)]$ or

$D^{(1)}=[5, 7, 4, 24]$, i.e., n = 4;

According to Eq. (18) $D^{(2)}$ can be found as:

$D^{(2)}=[2, -3, 20]$, i.e., n = 3.

Similarly, higher-order approximated derivatives can be determined utilizing the generic Eq. (18). However, the first, second, third, and fourth derivatives are used in the proposed methodology of XPQRS to signify the variation due to the disturbance event in a PQ signal.

3.2. Feature extraction

Feature extraction is a significant stage of PQ disturbance detection and classification framework. The objective is to identify the most decisive attributes with high discriminating ability between various PQ classes. Effective features have a great impact on the performance of a classification algorithm by highlighting the region of interest. To realize a PQ detection and classification algorithm on a real system, relevant features with high discriminating power having fewer dimensions are desirable. In this research, we employed a pool of features from time and spectral domains to identify the most capable descriptors after extensive experimental analysis. We propose a set of three features consisting of Log Energy (LE), Shannon Energy (SE), and Mobility (Mob) for classifying seven PQD classes. These features are extracted from the input signal and its four derivatives. The feature vector length becomes 15 in our case.

Let, the input vector to the feature extraction block is denoted by U, then these features are expressed mathematically as:

$$LE=\sum_{i=1}^{n} log(U_i^2), \tag{19}$$

$$SE=-\sum_{i=1}^{n} U_i^2 log(U_i^2), \tag{20}$$

and

$$Mob=\sqrt{\frac{Var\left(\frac{dU(t)}{dt}\right)}{Var(U(t))}} \tag{21}$$

For a comparative study, a wide range of discriminated features from two different domains were extracted from the original input voltage signal X as well as from the pre-processed signals $D^{(k)}$. Table 1 presents the time domain and spectral domain features respectively with their mathematical expressions [38–40]. Different combinations of features from each domain were fed to the classification block and the classification accuracy was analyzed. Feature from the two domains was fused and permutations from the resulting group of features were also tested for high accuracy and processing time. Extensive experimentation revealed that the features proposed for the PQ recognition system are powerfully connected to the problem.

3.3. Classification

The extracted feature vector from the previous step is given as input to various classifiers and the performance in each experiment

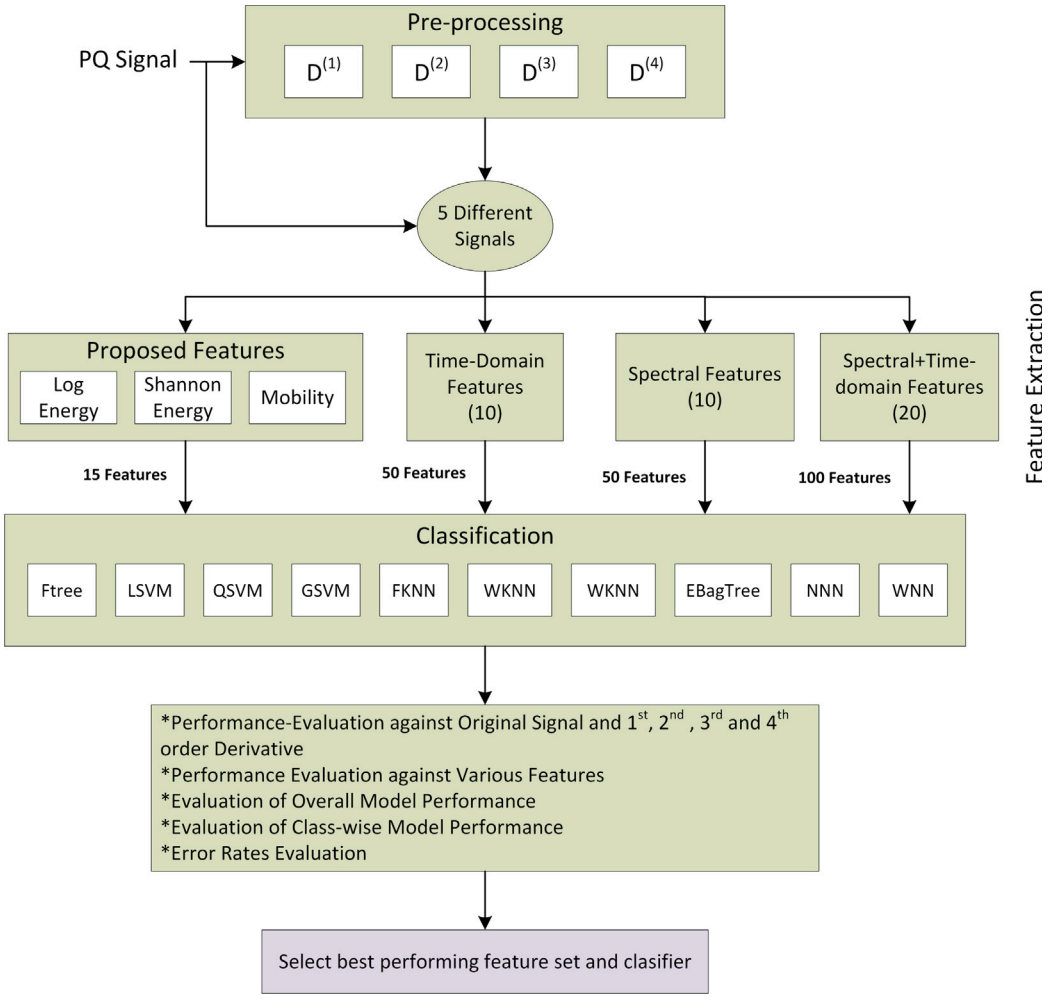

Fig. 2. Design of research for the proposed PQ disturbance recognition system.

Table 1
Time and spectral features with their mathematical representation used for comparison with the proposed features.

Time features	Equations	Spectral features	Equations
Peak to Peak	$PP = max(U) - min(U)$	Slope	$SSL = \frac{\sum_{k=b_1}^{b_2}(f_q-\mu_f)(s_q-\mu_s)}{\sum_{k=b_1}^{b_2}(f_q-\mu_f)^2}$
Mean	$U_{avg} = \frac{1}{n}\sum_{i=1}^{n} U_i$	Decrease	$SD = \frac{\sum_{q=b_1+1}^{b_2}\frac{s_q-s_{b1}}{q-1}}{\sum_{q=b_1}^{b_2} s_q}$
Kurtosis	$K = \frac{1}{n}\frac{\sum_{i=1}^{n}(U_i-U_{avg})^4}{\sigma^4}$	Flux	$SF = \left(\sum_{q=b_1}^{b_2}\lvert s_q(t) - s_q(t-1)\rvert^p\right)^{\frac{1}{p}}$
Crest factor	$CF = \frac{U_{peak}}{RMS}$	Skewness	$SS = \frac{\sum_{q=b_1}^{b_2}(f_q-\mu_1)^3 s_q}{\mu^3\sum_{q=b_1}^{b_2} s_q}$
Shape factor	$SF = \frac{RMS}{U_{am}}$	Centroid	$\mu_1 = \frac{\sum_{q=b_1}^{b_2} f_q . s_q}{\sum_{q=b_1}^{b_2} s_q}$
Impulse factor	$IF = \frac{U_{peak}}{U_{am}}$	Kurtosis	$SK = \frac{\sum_{q=b_1}^{b_2}(f_q-\mu_1)^4 s_q}{\mu^4\sum_{q=b_1}^{b_2} s_q}$
Margin factor	$MF = \frac{U_{peak}}{U_{am}^2}$	Spread	$SSP = \sqrt{\frac{\sum_{q=b_1}^{b_2}(f_q-\mu_1)^2}{\sum_{q=b_1}^{b_2} s_q}}$
Root mean square	$RMS = \sqrt{\frac{1}{n}\sum_{i=1}^{n}(U_i)^2}$	Roll off	$R = i \quad s.t. \sum_{q=b_1}^{i}\lvert s_q\rvert = k\sum_{q=b_1}^{b_2} s_q$
Skewness	$S = \frac{1}{n}\frac{\sum_{i=1}^{n}(U_i-U_{avg})^3}{\sigma^3}$	Crest	$SC = \frac{max(s_{q\in[b_1,b_2]})}{\frac{1}{b_2-b_1}\sum_{k=b_1}^{b_2} s_q}$
Standard deviation	$\sigma = \sqrt{\frac{\sum_{i=1}^{n}(U_i-U_{avg})^2}{n}}$	Flatness	$SFL = \frac{\left(\prod_{q=b_1}^{b_2} s_q\right)^{\frac{1}{b_2-b_1}}}{\frac{1}{b_2-b_1}\sum_{q=b_1}^{b_2} s_q}$

U_{am}: absolute mean of U and U_{peak}: peak value of U.
f_q: frequency (Hz) to bin q, s_q: spectral value at bin q, μ_s: mean spectral value, μ_f: mean frequency, p: the norm type, b_1 and b_2: band edges.

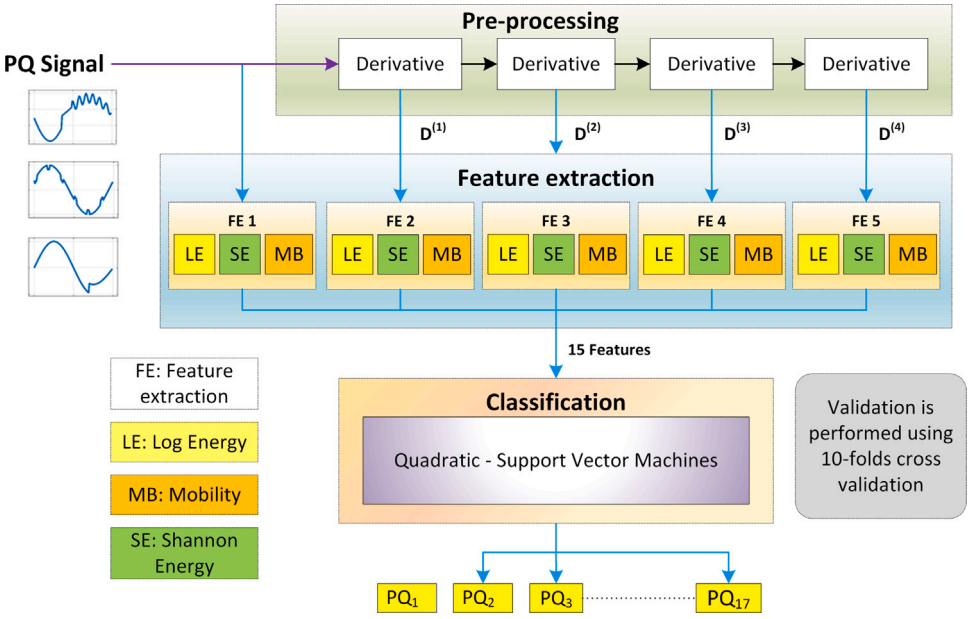

Fig. 3. The proposed Expert Power Quality Recognition System (XPQRS).

was critically analyzed. These classification algorithms include Fine Tree (Ftree), Support Vector Machine with the linear kernel (LSVM), SVM with Quadratic kernel (QSVM) [41,42], SVM with Gaussian kernel (GSVM) [43], Fine K-Nearest Neighbor classifier (FKNN), Weighted K-Nearest Neighbor (WKNN), Ensemble Boost Trees (EBooTree) Ensemble Bagged Trees (EBagTree), Nearest Neighbor Network (NNN) and Weighted Neighbor Network (WNN). The QSVM was selected for the proposed PQ identification scheme based on experimentation and high-end results.

SVM is a machine learning algorithm [42] that constructs an optimal segregating hyperplane by maximizing the margin between the hyperplane and class data [44,45]. It is used for the classification of different classes in a data set based on the variation of data related to each class [41,43]. Consider the classifier model training data is $F = \{f_1, \ldots, f_m\}$ which are the extracted features in our case, where $f_i \in R^m$ and class labels, $c_1, \ldots, c_m$ where $c_i \in -1, 1$. Let, $g(f) = 0$ be the hyperplane separating the input data then,

$$g(f) = w \times f + b = 0 \tag{22}$$

where w is an m-dimensional vector and b is a bias.

Considering the M-dimensional vector, $g(f)$ can be expressed as:

$$g(f) = \sum_{j}^{M} w_j f_i + b = 0 \tag{23}$$

SVM is required to maximize the separation margin between the classes. w and b parameters have a direct impact on the separation of the hyperplane.

$$c_i g(f) = c_i(w \times f + b) > +1 \quad if \quad c_i = 1 \tag{24}$$

$$c_i g(f) = c_i(w \times f + b) < +1 \quad if \quad c_i = -1 \tag{25}$$

By optimizing the geometrical distance i.e. $\|w\|^{-2}$ the optimal hyperplane can be obtained.

Minimize

$$min\varphi(w, d) = \frac{1}{2}\|w\|^2 + K\sum_{i=1}^{N} \psi_i \tag{26}$$

where d is a slack variable and K is a penalty factor.

Subject to

$$c_i(w \times f + b) \geq 1 - \psi_i \text{ for i=1, 2, 3, } \ldots, \text{ M} \tag{27}$$

$$\psi_i \geq 0 \text{ for all I} \tag{28}$$

The optimal bias values b

$$b = -\frac{1}{2}\sum_{SVMs} c_i\alpha_i * (\mu_1 * f_i + \mu_2 * f_i) \tag{29}$$

where μ_1 and μ_2 are random SVMs for c_1 and c_2, respectively.

α_i is a Lagrange multiplier, the non-zero values of f_i are known as support vectors. The decision function could be written as follows:

$$\sum_{SVMs} \alpha_i c_i f_i + b \tag{30}$$

Unidentified data is categorized as follows

$$f \in \begin{cases} c_1, & if\ g(x) \geq 0 \\ c_2, & otherwise \end{cases} \tag{31}$$

This feature vector is corresponding to a vector space which is generally a kernel function. The multi-class problem results in a non-linear basis which can be solved by applying a kernel function to the SVM model. There are different kernel functions such as linear, polynomial, Gaussian, and radial basis that can be used in SVM. In the proposed study, the quadratic polynomial is employed as a kernel function to classify PQ disturbances.

3.4. Proposed model: Expert Power Quality Recognition System (XPQRS)

As a result of the presented design of research, an expert system model for multi-complex PQ disturbance recognition is proposed in Fig. 3. One cycle of input PQ signal X is acquired and pre-processed using the first four derivatives i.e. $D^{(1)}$, $D^{(2)}$, $D^{(3)}$ and $D^{(4)}$. Then the discriminated features are extracted from the raw voltage signal as well as from $D^{(1)}$ through $D^{(4)}$ derivative signal. In this research, Log Energy (LE), Shannon Energy (SE), and Mobility (Mob) features are proposed based on experimentation. Then these feature values are made input to the QSVM classifier which classifies the 17 PQ disturbances with high accuracy.

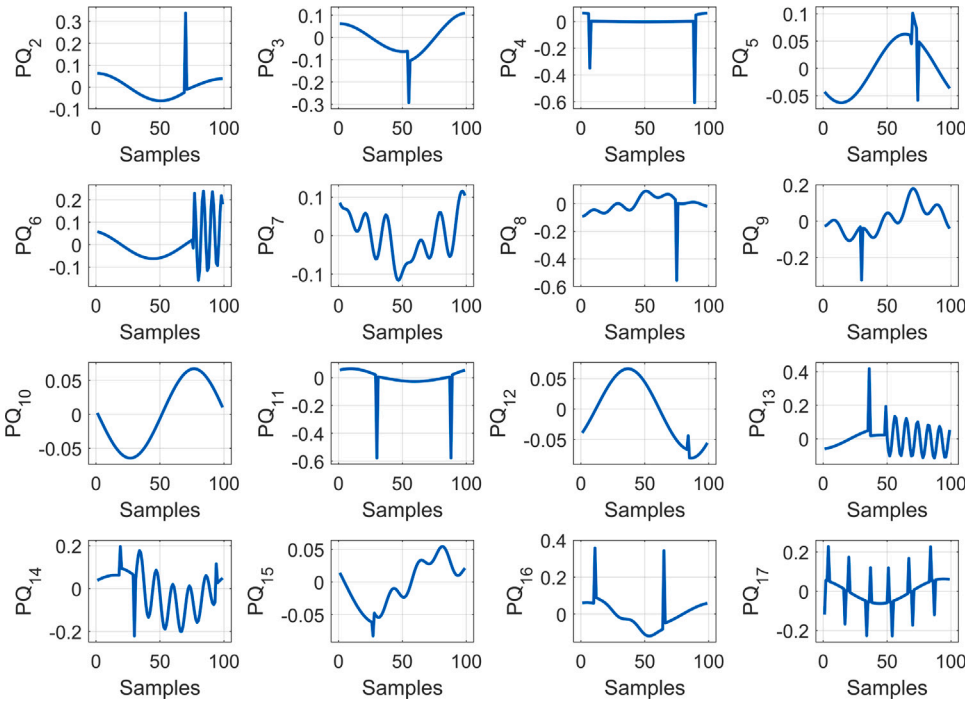

Fig. 4. Example waveforms for first derivatives of single cycle PQ disturbances used in this research.

4. Results and discussions

The majority of loads in the electrical network were not considered to be sensitive a few decades ago. Nowadays, ordinary load in electrical utility networks has been transmuted into sensitive load due to the integration of power electronic circuits. Motors are also sensitive to power quality disturbances as they have been converted into adjustable speed drives. Likewise, lighting load is now controlled by power electronic converters and has a tendency to be affected by a power disturbance. Many other loads have altered and become sensitive to PQ disturbances with the addition of power electronic switching circuits. The guidelines provided by IEEE standards related to the sensitive load reveal that preventive action must be taken in the minimum possible time to avoid any malfunction or damage to the sensitive load when a power disturbance occurs. The very first step to initiating the countermeasures is the detection and recognition of power quality disturbance. So, a high-speed preventive operation demands a fast and precise identification scheme. To design an efficient and high-performance expert system for PQ disturbance recognition that characterizes the disturbance class using only one cycle, there is a need for a pre-processing technique that can amplify the variations due to different PQ disturbances occurring in pure sine waves. Also, the highlighted deviations due to the pre-processing method can further be characterized using relevant features which may boost the performance of the classifier. Moreover, the use of a suitable classifier with such a combination of pre-processing methods and discriminated features will have a great impact on the overall performance of the classification system. To achieve these goals, a systematic procedure was built to find the combination of approximated derivatives in the pre-processing block, features in the feature extraction block, and classifier.

Figs. 4, 5, 6, and 7 show the first, second, third, and fourth-order derivatives respectively of these PQ events which depict that the disturbance shape and magnitude are now more noticeable in the waveform. Observing these derivative waveforms, it can be deduced that as we move towards the higher order approximated derivatives the sinusoidal (pure sine wave part) dies down and deviations in every type of PQ disturbance become more prominent.

The performance of the proposed methodology is evaluated through standard statistical measures of accuracy, sensitivity, and specificity utilizing True Positive (TP), True Negative (TN), False Positive (FP), and False Negative (FN) values. These metrics are defined as followed:

$$Accuracy = \frac{TP + TN}{TP + TN + FP + FN} \tag{32}$$

$$Sensitivity = \frac{TP}{TP + FN} \tag{33}$$

$$Specificity = \frac{TN}{TN + FP} \tag{34}$$

In this study, the k-fold cross-validation method was employed for training and testing each classifier. In the k-fold cross-validation method, the dataset is divided into k equal subsets. The classifier is trained on $k - 1$ signals in each subset of k signals and tested on the remaining signals. All results were computed using 10-fold cross-validation. The accuracies of the classifier against the test signal in each subset are averaged to yield an overall accuracy. In this study, each classifier was trained and assessed using 17 000 signals (1000 observations/class). The simulations were performed in MATLAB 2018 using a Core i5 computer with 8 GB RAM.

4.1. Results with an individual original input signal and its derivatives

The original signal and four approximated derivative signals were tested using various classifiers. Table 2 presents the accuracy results of these classifiers when the proposed feature extracted from original PQ signals was fed to them. In this experiment, the best results of 71% accuracy were obtained using EBagTree which is a type of ensemble classifier. The classwise accuracy or True Positive Rate (TPR) of the PQ_1 class which is pure sine wave is 100% for all classifiers. This shows the shape of the PQ_1 signal is very different than the rest of the PQ disturbance classes. All other classification algorithms attained

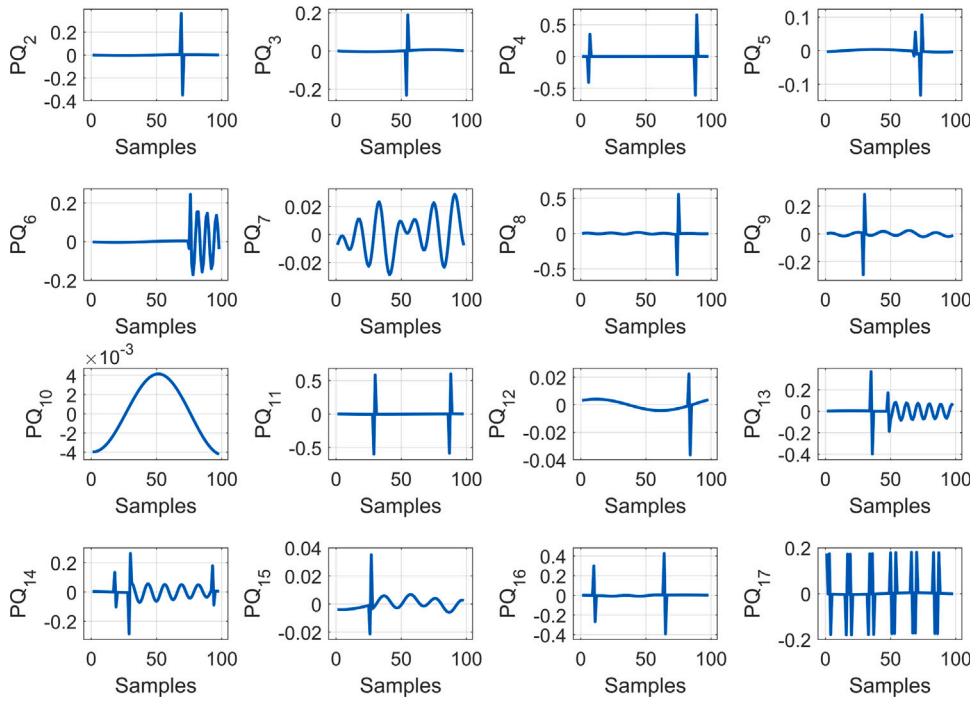

Fig. 5. Example waveforms for second derivatives of single cycle PQ disturbances used in this research.

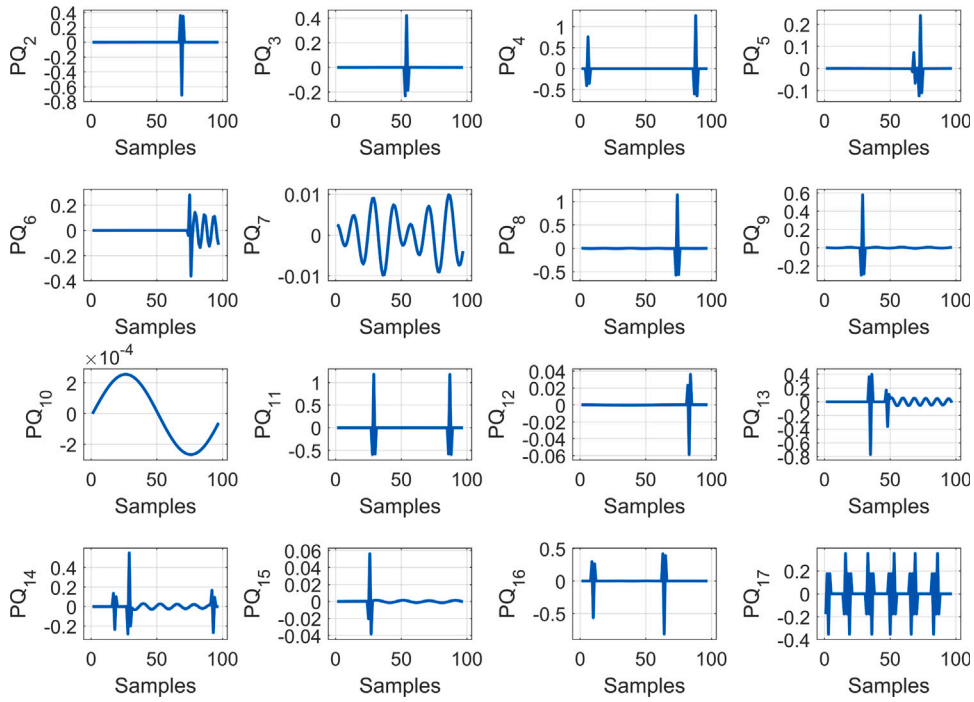

Fig. 6. Example waveforms for third derivatives of single cycle PQ disturbances used in this research.

comparatively low performance. It can be observed that the accuracies of each classification algorithm against individual disturbance classes are not up to the required levels in this particular scenario. The overall efficiencies of all the classifiers are very low. This depicts the complexity of the problem and leads us to devise a pre-processing technique that may support the classifier in distinguishing the PQ disturbances.

Table 3 provides the performance evaluation with first-order PQ signals (D_1) as input to the algorithm. Log energy, Shannon energy, and Mobility features were extracted from D_1 and passed to several classifiers. The performance of all employed classifiers was not satisfactory, as the best results of only 48.1% were obtained through the EBagTree classifier. All other classifiers provided low results. QSVM

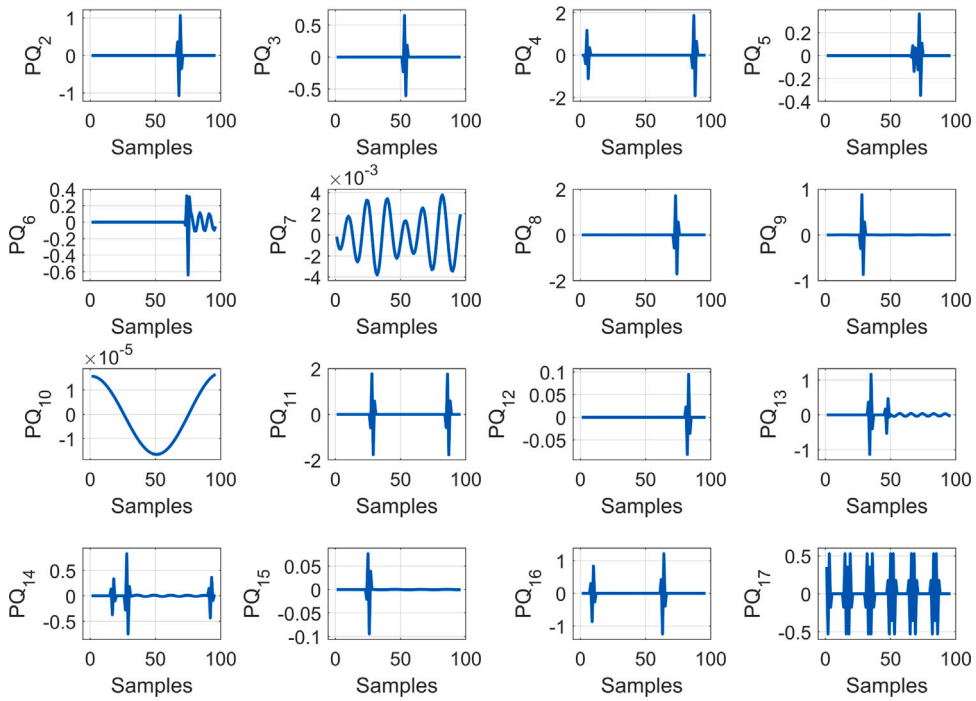

Fig. 7. Example waveforms for fourth derivatives of single cycle PQ disturbances used in this research.

Table 2
Accuracy results of different classifiers against proposed features extracted from original PQ signals.

Category	Classification methods								
	Ftree	LSVM	QSVM	FKNN	WKNN	EBooTree	EBagTree	NNN	WNN
PQ_1	100.0	100.0	100.0	100.0	100.0	100.0	100.0	100.0	100.0
PQ_2	50.7	72.7	78.3	77.0	84.0	89.0	83.3	84.0	90.3
PQ_3	88.7	93.3	94.3	93.3	95.0	82.0	96.0	92.3	94.7
PQ_4	86.7	84.7	89.7	91.7	93.0	81.7	93.3	85.7	95.0
PQ_5	96.7	95.7	97.0	82.7	92.7	99.7	94.3	95.7	96.3
PQ_6	64.7	68.7	71.0	71.3	72.3	64.7	76.3	68.7	75.3
PQ_7	89.7	86.3	90.7	82.7	87.3	67.0	88.0	90.7	89.3
PQ_8	43.7	16.7	19.7	94.3	35.7	1.3	41.7	43.7	47.0
PQ_9	50.0	49.3	46.0	44.3	46.3	69.7	54.0	53.0	53.0
PQ_{10}	99.3	99.7	99.3	98.0	99.0	98.3	99.7	99.3	99.0
PQ_{11}	12.0	35.0	35.0	33.3	32.3	2.0	33.0	17.0	27.7
PQ_{12}	52.0	54.7	67.0	46.3	51.7	41.3	53.7	60.3	65.0
PQ_{13}	47.3	66.3	65.7	62.7	63.0	55.3	66.7	70.0	67.7
PQ_{14}	76.7	69.3	72.3	70.0	69.7	64.0	74.7	74.3	74.0
PQ_{15}	33.7	40.7	52.7	36.0	41.7	0.0	38.3	42.7	37.7
PQ_{16}	14.3	39.7	21.3	33.3	35.0	1.0	32.7	20.3	30.7
PQ_{17}	77.7	74.7	85.3	74.0	83.0	86.0	82.0	81.3	82.7
Overall	**63.7**	**67.5**	**69.7**	**66.5**	**69.5**	**59.0**	**71.0**	**69.4**	**72.1**

classifier reached 43% overall accuracy, with TPRs of 100%, 86%, and 84% for PQ_1, PQ_4, and PQ_5, respectively. It failed to predict the PQ_3, PQ_6, PQ_{11}, and PQ_{12} signals. These results indicate that first derivate PQ signals hold weak discriminant information required to classify different disturbances.

Results of testing second derivative PQ signals with the proposed features and various classifiers are illustrated in Table 4. 59.6% accuracy of classification was achieved via the EBagTree ensemble classifier. It was observed that the QSVM classifier obtained a TPR of 100% for PQ_1, PQ_7, and PQ_{10}. The overall accuracy of only 31.6% was obtained through QSVM.

Table 5 enlists experimental evaluation of all employed classifiers with proposed features using the third derivative of PQ signals. The most suitable results of 60.4% accuracy were obtained using the EBagTree classifier. Ftree, LSVM, and EBooTree provided 55.7%, 45.4%, and 52.5% accuracies, respectively. In the case of QSVM, only PQ_4, PQ_7, and PQ_{10} classes have enhanced results. These classifiers have failed to predict other PQ classes with substantial accuracy.

The fourth derivative of the PQ signal was also tested individually with the proposed features and several classification algorithms. Table 6 illustrates these experimental details. The best results of 64.2% were obtained in this experiment via the EBagTree classifier. Notable performances of 56.9% and 64.2% were provided by the Ftree and EBagTree classifiers, respectively. There are only a few PQ disturbances for which the derivative signals have enhanced the performance of

Table 3
Accuracy results of different classifiers against proposed features extracted from $D^{(1)}$ of PQ signals.

Category	Classification methods								
	Ftree	LSVM	QSVM	FKNN	WKNN	EBooTree	EBagTree	NNN	WNN
PQ_1	100.0	0.0	100.0	100.0	100.0	100.0	100.0	100.0	100.0
PQ_2	19.7	35.0	26.0	33.7	34.7	29.3	38.0	30.3	34.0
PQ_3	37.3	0.0	0.7	28.0	30.0	12.7	33.3	49.3	50.7
PQ_4	83.0	74.7	86.0	86.0	87.3	75.3	92.7	90.3	88.7
PQ_5	73.3	69.0	84.7	58.3	67.0	53.7	81.3	82.3	81.0
PQ_6	44.3	12.0	0.0	18.3	19.7	22.7	26.0	22.0	25.0
PQ_7	94.3	92.7	99.0	75.3	87.3	89.0	92.0	93.0	96.0
PQ_8	13.7	19.0	15.0	16.0	14.0	17.3	26.7	14.0	18.0
PQ_9	44.0	24.7	41.7	19.3	20.0	4.0	24.7	25.0	28.7
PQ_{10}	98.7	97.7	99.7	98.3	98.7	100.0	99.0	69.3	61.0
PQ_{11}	26.7	0.3	2.0	13.3	14.3	0.0	20.7	18.7	21.7
PQ_{12}	26.0	10.3	0.0	15.7	17.7	28.3	24.0	12.7	16.7
PQ_{13}	15.3	30.7	19.7	20.3	19.7	2.0	29.3	19.7	21.0
PQ_{14}	13.0	31.3	45.3	21.0	21.0	65.7	21.7	19.0	26.7
PQ_{15}	2.0	0.3	19.0	13.3	12.7	0.0	20.7	8.0	9.3
PQ_{16}	5.3	0.0	18.7	10.3	10.3	0.0	13.0	3.3	10.3
PQ_{17}	54.3	59.0	73.0	66.7	66.0	50.7	74.3	64.7	63.7
Overall	**44.2**	**32.7**	**43.0**	**40.8**	**42.4**	**38.3**	**48.1**	**42.5**	**44.3**

Table 4
Accuracy results of different classifiers against proposed features extracted from $D^{(2)}$ of PQ signals.

Category	Classification methods								
	Ftree	LSVM	QSVM	FKNN	WKNN	EBooTree	EBagTree	NNN	WNN
PQ_1	100.0	100.0	100.0	100.0	100.0	100.0	100.0	100.0	100.0
PQ_2	16.3	32.7	0.0	31.0	29.7	20.0	40.7	27.0	22.3
PQ_3	59.3	0.0	0.0	29.3	32.0	74.3	43.7	29.7	41.7
PQ_4	95.0	85.7	92.0	84.3	88.0	84.0	94.0	87.3	91.3
PQ_5	89.3	39.0	0.0	58.7	64.7	91.7	86.3	89.3	86.7
PQ_6	58.7	64.0	0.0	33.0	37.7	58.7	55.3	64.7	52.0
PQ_7	100.0	100.0	100.0	98.0	99.3	100.0	100.0	100.0	100.0
PQ_8	3.3	0.0	0.0	14.3	13.3	0.0	23.0	0.0	3.3
PQ_9	49.3	38.3	0.0	20.7	26.3	13.3	94.7	31.0	50.3
PQ_{10}	100.0	100.0	100.0	93.0	99.3	100.0	99.7	100.0	100.0
PQ_{11}	27.0	0.0	1.0	20.7	20.0	13.7	32.7	5.7	18.0
PQ_{12}	0.3	0.0	0.0	24.3	26.0	0.0	38.7	21.0	22.0
PQ_{13}	16.7	13.7	43.0	26.0	24.3	39.3	39.0	10.7	21.7
PQ_{14}	41.0	29.7	48.7	25.0	29.0	8.0	32.3	29.7	38.0
PQ_{15}	4.3	49.7	0.0	15.0	12.7	0.0	21.7	3.0	3.0
PQ_{16}	0.0	21.7	0.0	16.3	16.3	0.0	18.0	1.3	13.7
PQ_{17}	73.0	37.0	52.7	79.0	81.7	60.0	92.7	75.7	82.3
Overall	**49.0**	**41.9**	**31.6**	**45.2**	**47.1**	**44.9**	**59.6**	**45.7**	**49.8**

Table 5
Accuracy results of different classifiers against proposed features extracted from $D^{(3)}$ of PQ signals.

Category	Classification methods								
	Ftree	LSVM	QSVM	FKNN	WKNN	EBooTree	EBagTree	NNN	WNN
PQ_1	100.0	100.0	0.0	100.0	100.0	100.0	100.0	100.0	100.0
PQ_2	32.0	44.8	0.0	18.5	19.0	32.2	49.0	27.5	21.0
PQ_3	40.8	41.2	0.0	29.0	28.7	85.2	58.2	41.2	39.5
PQ_4	86.8	83.0	95.0	72.2	72.2	84.8	94.2	77.8	79.2
PQ_5	88.0	48.2	0.0	82.5	85.0	87.8	93.0	83.5	84.2
PQ_6	81.2	44.8	13.2	32.8	38.0	87.2	59.0	50.5	50.5
PQ_7	100.0	100.0	100.0	100.0	100.0	100.0	100.0	100.0	100.0
PQ_8	9.0	16.8	0.2	20.0	20.8	0.0	26.0	24.0	15.8
PQ_9	64.8	62.3	28.2	50.7	55.8	81.2	58.2	64.2	70.0
PQ_{10}	99.5	79.8	100.0	98.0	99.2	99.8	98.5	60.8	83.5
PQ_{11}	29.8	5.8	0.0	18.5	18.5	9.2	30.5	21.0	13.5
PQ_{12}	13.0	3.8	49.2	17.5	19.0	12.2	37.2	3.5	18.8
PQ_{13}	16.2	12.5	31.8	18.5	22.0	3.5	30.0	3.2	31.0
PQ_{14}	20.8	24.2	33.0	20.2	22.2	19.0	36.0	43.0	23.5
PQ_{15}	29.0	23.0	0.0	14.8	15.8	0.0	33.0	9.8	11.5
PQ_{16}	44.2	22.0	0.0	19.5	20.2	0.0	27.0	24.8	28.2
PQ_{17}	91.8	60.0	92.8	56.0	57.0	90.8	96.8	55.0	53.0
Overall	**55.7**	**45.4**	**32.0**	**45.2**	**46.7**	**52.5**	**60.4**	**46.5**	**48.8**

Table 6
Accuracy results of different classifiers against proposed features extracted from $D^{(4)}$ of PQ signals.

Category	Classification methods								
	Ftree	LSVM	QSVM	FKNN	WKNN	EBooTree	EBagTree	NNN	WNN
PQ_1	100.0	100.0	0.0	100.0	100.0	100.0	100.0	100.0	100.0
PQ_2	11.0	50.0	2.0	24.0	23.2	2.2	52.2	37.0	8.5
PQ_3	55.2	3.8	0.0	24.2	25.5	75.0	65.0	29.2	48.5
PQ_4	78.8	80.0	98.8	75.0	77.0	79.0	92.0	85.0	79.0
PQ_5	87.5	8.2	0.0	82.2	83.8	91.0	93.2	75.2	86.2
PQ_6	73.5	22.8	4.8	34.5	37.0	58.5	66.5	69.0	50.7
PQ_7	100.0	100.0	100.0	100.0	100.0	100.0	100.0	100.0	100.0
PQ_8	10.0	31.5	92.8	27.8	27.0	1.8	34.8	32.5	22.5
PQ_9	83.0	60.2	0.0	53.8	56.5	88.0	66.2	75.2	75.2
PQ_{10}	100.0	100.0	100.0	94.5	98.5	99.8	100.0	99.5	99.5
PQ_{11}	26.0	0.0	0.0	20.8	20.2	23.5	37.5	7.8	22.0
PQ_{12}	30.8	57.5	0.0	22.5	23.8	0.0	44.5	10.8	23.0
PQ_{13}	35.5	12.0	3.0	17.2	18.8	0.0	34.0	5.2	22.2
PQ_{14}	21.2	21.5	57.5	18.8	18.5	17.5	32.0	7.0	23.5
PQ_{15}	45.0	11.2	0.2	24.2	24.8	38.5	40.5	26.2	29.5
PQ_{16}	30.0	47.2	0.0	24.2	27.3	28.5	37.5	30.8	33.2
PQ_{17}	80.5	23.5	0.0	57.8	61.3	87.5	95.5	29.2	61.3
Overall	**56.9**	**42.9**	**27.0**	**47.1**	**48.4**	**52.4**	**64.2**	**48.2**	**52.1**

Table 7
Accuracy results of different classifiers against proposed features extracted from original PQ signals, $D^{(1)}$, $D^{(2)}$, $D^{(3)}$, and $D^{(4)}$.

Category	Classification methods								
	Ftree	LSVM	QSVM	FKNN	WKNN	EBooTree	EBagTree	NNN	WNN
PQ_1	100.0	100.0	**100.0**	100.0	100.0	100.0	100.0	100.0	100.0
PQ_2	85.3	89.8	**98.2**	97.3	97.3	82.0	96.8	93.7	98.4
PQ_3	76.8	96.4	**99.3**	99.2	99.1	73.8	99.3	99.0	99.5
PQ_4	84.7	95.6	**96.4**	97.6	97.7	90.3	98.8	97.0	98.9
PQ_5	93.6	96.7	**97.3**	97.2	97.8	96.4	98.2	96.0	97.3
PQ_6	85.9	90.4	**95.9**	85.2	91.2	86.5	93.0	93.7	92.3
PQ_7	100.0	100.0	**100.0**	100.0	100.0	100.0	100.0	99.9	99.8
PQ_8	61.2	95.7	**96.8**	87.7	91.1	54.2	94.9	95.8	94.8
PQ_9	87.6	96.6	**97.5**	91.9	94.6	88.7	96.3	97.0	96.7
PQ_{10}	100.0	100.0	**100.0**	99.8	100.0	100.0	99.8	99.9	100.0
PQ_{11}	52.2	85.2	**94.9**	80.9	76.9	27.1	89.0	85.2	90.2
PQ_{12}	92.2	96.3	**97.8**	93.8	94.3	81.1	97.1	97.5	96.5
PQ_{13}	78.1	82.4	**89.0**	78.9	73.7	74.7	87.3	87.4	90.0
PQ_{14}	81.0	79.6	**90.7**	78.8	73.3	72.0	88.1	89.7	90.7
PQ_{15}	63.1	85.2	**92.0**	85.7	84.3	62.8	88.0	87.3	92.0
PQ_{16}	79.3	92.4	**96.0**	85.9	85.1	73.7	91.5	91.8	94.6
PQ_{17}	92.7	95.8	**98.3**	98.7	98.1	91.0	97.9	95.7	98.6
Overall	**83.2**	**92.8**	**96.5**	**91.7**	**91.4**	**79.7**	**95.1**	**94.5**	**95.9**

some classifiers. Experimental analysis suggested that the overall performance of all classifiers is not encouraging when $D^{(1)}$, $D^{(2)}$, $D^{(3)}$ and $D^{(4)}$ derivatives were utilized separately. It also points to the complex nature of data where separation using only a limited set of features is a challenging task.

4.2. Results using a combination of the original signal and first four derivatives

Experimental analysis indicated that the best performance for the classification of PQ disturbance signals was obtained through a combination of the original signal and its first four derivatives, followed by feature extraction from all five signals. Three features namely, log energy, Shannon energy, and Mobility were extracted from all five input signals. The feature vector of 1×15 is constructed to train and test a range of classification methods. Table 7 shows the evaluation results of the classifiers when the original PQ signals and $D^{(1)}$, $D^{(2)}$, $D^{(3)}$ and $D^{(4)}$ of PQ signals were employed instead of individual derivatives. The best performance of 96.5% overall accuracy was attained using the QSVM classifier. All classes in this case achieved TPR of more than 90%. EBagTree, WNN, NNN, and LSVM provided 95.1%, 94.5%, 95.9%, and 92.8%, respectively. High accuracy results of all the classifiers are evidence of the advantage of using the four approximated derivatives with raw PQ signal. Although the accuracy of each classifier is improved by adopting this strategy, however, QSVM exhibits the highest overall accuracy of 96.5% in recognizing 17 single and composite PQ disturbance classes.

Fig. 8a shows a 17×17 confusion matrix illustrating the capability of a correct decision of the proposed method. The diagonal values give the correct classification of PQ events, and other than diagonal elements represent the miss-classified PQ disturbances. Fig. 8b provides the confusion matrix in terms of percentage accuracy. All 1000 observations of PQ_1, PQ_7, and PQ_{10} classes were correctly predicted, hence, sensitivity values of 100% were achieved for these categories. Out of a total of 1000 observations of PQ_{13} (Sag with Oscillatory Transient), 890 were correctly classified, however, the classification model mispredicted 36 PQ_{13} observations as PQ_6 (Oscillatory Transient) and 41 as PQ_{11} (Flicker with Sag). The TPR of the PQ_{13} class was 89%, making it the lowest among all other categories. These reduced results were due to the fact that both PQ_{13} and PQ_6 signals contain oscillatory transients, making it challenging for the classifier to differentiate. The proposed framework is still capable of delivering excellent classification results, with only one class below the 90% range. All other PQ events obtained well above 90% TPRs. Results presented in Tables 2–7 confirm that the

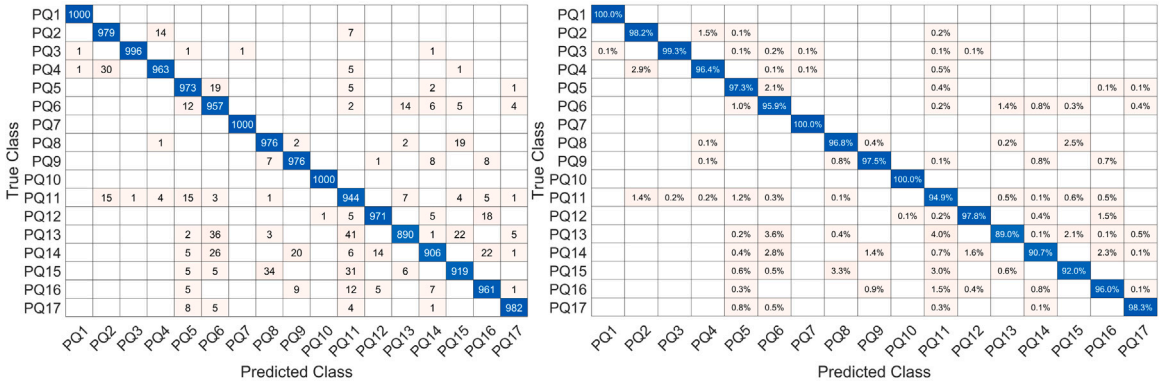

(a) Confusion matrix in terms of number of observations. (b) Confusion matrix in terms of percentages.

Fig. 8. Confusion matrices illustrating the capability of the correct decision of the proposed method in classifying 17 PQ classes.

Table 8
Performance comparison of proposed features with time and spectral features extracted from (original + $D^{(1)} + D^{(2)} + D^{(3)} + D^{(4)}$) in recognizing PQ disturbances.

Feature type	Time features (50)	Spectral features (50)	Time + Spectral (100)	Proposed features (15)
Ftree	79.8%	76.1%	86.2%	83.2%
LSVM	83.8%	91.6%	91.9%	92.8%
QSVM	90.5%	92.5%	93.8%	96.5%
FKNN	80.2%	84.5%	87.9%	91.7%
WKNN	79.3%	85.1%	88.0%	91.4%
EBooTree	72.1%	79.8%	83.4%	79.7%
EBagTree	90.9%	92.2%	93.5%	95.1%
NNN	87.0%	92.2%	93.8%	94.5%
WNN	91.7%	92.8%	93.5%	95.9%

proposed method using a combination of the original PQ signal and its derivatives has better recognition ability.

4.3. Performance comparison of proposed features with time and spectral features

Training and testing of various classification algorithms were carried out using 50 features from the time and spectral domain. The same was done by concatenating the features from both domains. The results were compiled in Table 8. It can be seen from the tabled data that even a large number of features could not yield satisfactory performance as compared to the proposed features. Although EBagTree, NNN, WNN, and QSVM exhibit accuracies higher than 90%, due to a large number of features in the group containing time and spectral descriptors. These combinations of features and classifiers increase the computational complexity of the classification scheme. As a result, more hardware resources will be required while realizing these combinations on real systems. The proposed PQ identification method uses a set of three simple features extracted from all five preprocessed signals with QSVM, which makes this combination favorable for real scenarios.

4.4. Performance comparison of XPQRS with state-of-the-art

It is evident from Table 9, that the proposed XPRS provides an appropriate success. It can be deduced from the relevant IEEE standards that the classification of PQD and the preventive procedure must be completed in a time multiple of milliseconds to avoid any maloperation or damage to the sensitive load. So, the time window for detection and classification is very narrow according to this scenario. To deal with this challenge, the computational complexity of the PQD identification scheme is significantly reduced by using only one cycle of the input voltage signals and a very lower sampling frequency. As a result, the proposed PQD classification algorithm offers a very small execution time.

Table 10 gives the execution time of pre-processing step, feature extraction step, and classification step of the proposed classification system in identifying the 17 single-cycle PQ disturbances. These simulations were performed using a platform comprising a personal computer having a Core i5 processor with 8 GB RAM. MATLAB's *tic-toc* function was utilized for the execution time of each processing step. The pre-processing, feature extraction, and classification take average execution time of 0.485 ms, 0.781 ms, and 32.560 ms respectively in detecting all the classes. The overall processing time of the proposed algorithm is 34.99 ms. This shows that the proposed pre-processing and feature extraction technique has positive repercussions on the processing speed of the detection scheme. The fundamental preferred standpoint of the proposed method is low execution time and noteworthy precision.

Table 11 compares the execution time of the proposed method with previous works. The proposed method has less prediction time. However, it is pertinent to mention that the overall performance of an algorithm is influenced by several other factors, such as computational power, sampling frequency, number of signals classified, classifier type, and processor speed and complexity of individual stages of the algorithm [46]. In most of the previous works, only testing times were reported [46,47]. For efficient implementation of a real-time PQD monitoring system, the computation/processing time should be less than the time period of one cycle, i.e., 20 ms, so that the processing on one window/frame is completed before the arrival of new data/frame. The results reported in this study are based on a simulation and obtained using software simulations on a PC. Generally, it is observed that the processing time of a PQ classification algorithm is long when it is implemented in software simulation on a PC because of the fact that the resources of the computer are occupied and busy doing tasks related to the operating system and other applications. Authors in [7,48] reported a considerable reduction in processing time when they implemented the PQ detection and classification methods on hardware. The proposed XPQRS provides another edge in implementing the algorithm on digital/embedded architectures. The feature descriptor proposed in this work only consists of three features, and the same sets of descriptors

Table 9
Comparison of XPQRS with the previous studies in terms of number of classes, accuracy, number of cycles per PQ signal, and sampling rate.

References	Method	No. of classes	Accuracy%	No. of cycles	Sampling frequency (kHz)
[8]	WPT, SVM	8	98.3	12	12.5
[9]	EMD, ANN	9	100	–	20.48
[10]	CS, DCNN	15	99	10	–
[11]	SWT, NN	10	94.7	10	200
[12]	ST	15	99	10	6.4
[13]	MST	8	100	10	15.36
[15]	HoS, NT	20	97	–	–
[16]	FEFS, MC-SVM	9	98.65	20	–
[17]	DWT, ELM	6	100	10	10
[18]	PSO, ELM	10	97	10	12.8
[19]	DWT, O-SVM	5	93	10	–
[20]	DWT, CC	9	98.17	15	20
[21]	IPCA, 1D-CNN	12	99.92	10	10
[22]	FTDD, MSVM, NB	6	99	10	
[23]	STF, ELM	20	92.6	10	6.4
[24]	DWT, H-ELM	15	95	10	6.4
[25]	DWT and ANN	6	100	10	6.4
[26]	St-T, DT	9	–	15	3.2
[27]	TF, DT	12	99.9	1 sec	3.2
[28]	MST, DT	16	99	1 sec	3.2
[29]	ST, rule-based DT	7	99.4	10	3.2
[30]	MST, PSSAE	13	99.06	10	2.56
[31]	DRST, DAG-SVM	9	80	10	5
[32]	VMD, DSCN	7	99.4	10	2
[33]	VMD, ST,SVM	9	99.66	10	3.2
[34]	SVECP	10	99.38	10	2
[35]	LSTM, RNN	9	98.7	15	1
[36]	CCWTC	5	99.8	8	25.6
XPQRS (Our work)	Derivatives, LE, SE, Mob, QSVM	17	96.5%	1	5

Table 10
Stage-wise timing analysis of the proposed scheme.

Input class	Pre-processing (ms)	Feature extraction (ms)	Classification (ms)	Total time (ms)
PQ_1	0.591	1.402	32.604	34.597
PQ_2	0.218	0.396	33.725	34.339
PQ_3	0.475	0.544	33.153	34.172
PQ_4	0.536	0.836	33.431	34.803
PQ_5	0.538	0.887	32.109	33.534
PQ_6	0.297	0.756	33.406	34.459
PQ_7	1.845	1.571	33.945	37.361
PQ_8	0.588	0.78	34.166	35.534
PQ_9	0.424	0.602	34.248	35.274
PQ_{10}	0.652	0.835	32.56	34.047
PQ_{11}	0.022	0.236	33.669	33.927
PQ_{12}	0.031	0.238	35.201	35.47
PQ_{13}	0.32	0.482	35.587	36.389
PQ_{14}	0.69	1.099	33.437	35.226
PQ_{15}	0.021	0.225	34.524	34.77
PQ_{16}	0.967	1.083	34.21	36.26
PQ_{17}	0.023	0.234	34.552	34.809
Average	0.485	0.718	33.796	34.999

Table 11
Comparison of the execution time of the proposed method with various studies.

Reference	Total execution time (ms)
[49]	176.2
[50]	63.3
[46]	83.4
[47]	37
XPQRS (This work)	34.99

are extracted from all PQ signals and their four derivatives. This enables digital designers to copy the same architecture and process the signals in parallel. This capability will further reduce the computation time once the system is implemented on hardware.

4.5. Performance of the XPQRS on various noise levels

In a real-world setting, noise typically superimposes itself on sensor signals [51]. Power electronic drives, control circuits, arcing devices, loads with solid-state rectifiers, and switching power supplies can all contribute to noise in the electric power system. The noise level of real PQD waveforms in an electrical system is approximately 45 dB [52,53]. However, the resilience of the proposed XPQRS was also evaluated under more tough noisy conditions. For that purpose, additive white Gaussian noise (AWGN) was added to PQD signals with a signal-to-noise ratio (SNR) ranging from 30 dB to 60 dB. These noisy test signals were used for the performance evaluation of XPQRS under noisy conditions. This gives an insight into the ability of the scheme for working satisfactorily if implemented on a real system.

Fig. 9 shows the detection accuracy of the proposed method under noisy conditions, which renders the fact that the accuracy remains nearly unaffected up to 30 dB. The accuracy results with 30 dB, 40 dB, 50 dB, and 60 dB noise are 93.31%, 93.33%, 93.9%, and 94.9%, respectively. However, as input noise interference grows, the classifier's performance degrades. The proposed classification scheme shows appreciably good noise immunity against the single PQD classes. However, it is noticed that the method presents a comparatively reduced

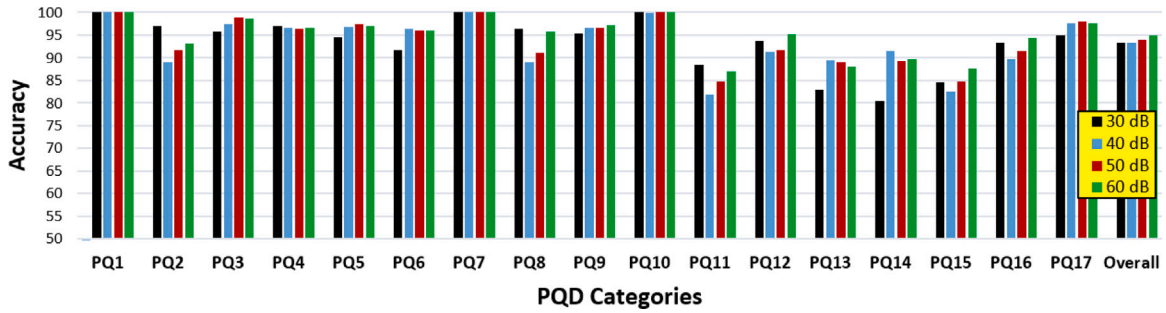

Fig. 9. Performance of XPQRS with PQ signals having 30 dB, 40 dB, 50 dB, and 60 dB noise.

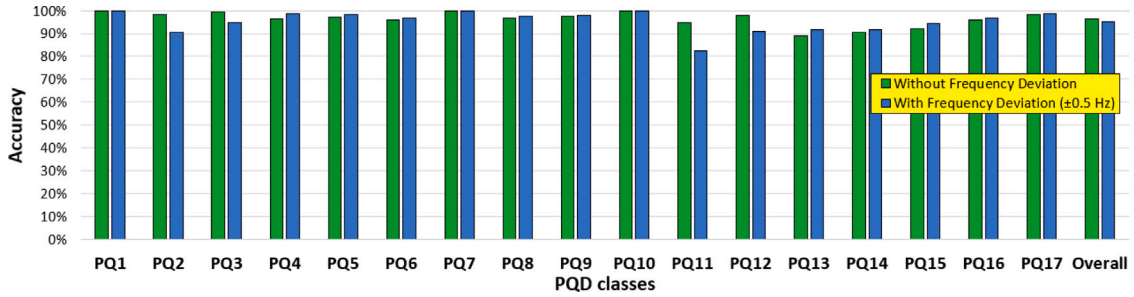

Fig. 10. Performance of XPQRS with and without frequency deviation.

yet satisfactory performance in the case of hybrid (multi-complex) disturbance events i.e. PQ_8, PQ_9, PQ_{11}, PQ_{12}, PQ_{13}, PQ_{14}, PQ_{15}, and PQ_{16}. These erroneous classifications are closely related to the fact that derivatives (noise enhancers) are being used in the pre-processing stage of XPQRS. Despite that, it is observed that the methodology has a satisfactory performance even when faced with noise that mischaracterizes the signal with a low sampling rate, and only one cycle that provides little information about the disturbances.

4.6. Performance of the XPQRS against source frequency deviations

There are various reasons for fluctuations in power line frequency, including changes in demand for electricity, power generation variations, and disturbances in the power grid. The permissible frequency fluctuation of power sources depends on the type of electrical system, the country, and the application. Most countries have established standards for allowable frequency deviation in their electrical systems. The European Network of Transmission System Operators for Electricity (ENTSO-E), sets standards for the frequency of the interconnected power grid in Europe, which should be maintained within a range of 49.8 to 50.2 Hz [54].

To validate the proposed XPQRS, its performance was assessed on PQD signals that had frequency fluctuations. A new dataset of PQD classes was created, which had 3000 observations in each class, with three frequencies, i.e., 49.5, 50, and 50.5 Hz. The proposed method demonstrated a good overall accuracy of 95.4% against PQ signals with frequency deviation higher than the permissible range of ENTSO-E standard. The comparative analysis of the proposed method with and without frequency deviation is shown in Fig. 10. Although there was a slight 1.10% drop in the overall performance, the experimental analysis showed that the proposed features and classifier combination did not completely fail to recognize any disturbance. The PQ_{11} class had the lowest classwise accuracy of 82.40%, which still fell within the acceptable range.

5. Conclusions and recommendations

This research presents an expert system for the PQ disturbance recognition system (XPQRS) to identify seventeen PQD events (eight single and nine hybrids). The proposed strategy utilizes only one cycle acquired at a 5 kHz sampling rate to classify the PQ disturbance. The XPQRS employs the original signal with its first four approximated derivatives and powerful discriminative features like Log Energy, Shannon Energy, and Mobility to characterize the change upon the occurrence of PQ events. The overall performance of XPQRS is 96.5% which is very encouraging with respect to complexity and time constraints imposed by sensitive load requirements. A small number of features restrains the computational burden and reduces execution time for disturbance recognition. Moreover, the use of one cycle window size with the proposed features has made it possible to achieve a very short processing time of 34.99 ms. The main attributes of the proposed system are accurate operation, reliability, robustness against noisy conditions, and easy implementation on real-time embedded architectures. Consequently, XPQRS can be helpful in resolving the issues faced in protection systems for sensitive load applications such as high-power electronics, static transfer switches, and smart grids.

However, the pre-processing derivative functions as a high pass filter and may enhance the noise under highly noisy conditions. The proposed approach may show reduced performance in case of missing data, non-linear loads, harmonic contamination of PQ signals, and under uncertainties. In the future, PQ issues will be more intricate than those described in this article because renewable energy penetration will increase to a new peak. The proposed XPQRS system can be further improved by including more hybrid, complex, and real PQ disturbances. There is room for PQ analytics technology to advance, particularly for real-time PQ events. The authors intend to embed an integration of XPQRS with low-cost hardware for the timely identification of PQ disturbance. In this way, measures can be taken to protect sensitive equipment from damage.

CRediT authorship contribution statement

Muhammad Umar Khan: Conceptualization, Methodology, Software, Data curation, Formal analysis, Writing – original draft. **Sumair Aziz:** Methodology, Software, Investigation, Data curation, Writing – original draft, Writing – review & editing. **Adil Usman:** Conceptualization, Validation, Supervision, Writing – original draft, Writing – review & editing.

Declaration of competing interest

The authors declare that they have no known competing financial interests or personal relationships that could have appeared to influence the work reported in this paper.

Data availability

Data will be made available on request.

References

[1] P.R. Babu, P. Dash, S. Swain, S. Sivanagaraju, A new fast discrete S-transform and decision tree for the classification and monitoring of power quality disturbance waveforms, Int. Trans. Electr. Energy Syst. 24 (9) (2014) 1279–1300.

[2] I.S. Association, et al., IEEE recommended practice for monitoring electric power quality, 2009.

[3] B. Standard, et al., Voltage characteristics of electricity supplied by public distribution networks, BS EN (2007).

[4] A. Thapar, T.K. Saha, Z.Y. Dong, Investigation of power quality categorisation and simulating it's impact on sensitive electronic equipment, in: IEEE Power Engineering Society General Meeting, 2004, IEEE, 2004, pp. 528–533.

[5] G.F. Reed, M. Takeda, I. Iyoda, Improved power quality solutions using advanced solid-state switching and static compensation technologies, in: IEEE Power Engineering Society. 1999 Winter Meeting (Cat. No. 99CH36233), Vol. 2, IEEE, 1999, pp. 1132–1137.

[6] A. Usman, M.A. Choudhry, An efficient and high-speed disturbance detection algorithm design with emphasis on operation of static transfer switch, Adv. Electr. Comput. Eng. 21 (2) (2021) 87–98.

[7] A. Usman, M.A. Choudhry, Hardware realization of an innovative disturbance detection algorithm for control strategy of solid-state transfer switch, IEEE Trans. Ind. Electron. (2022).

[8] K. Manimala, K. Selvi, R. Ahila, Optimization techniques for improving power quality data mining using wavelet packet based support vector machine, Neurocomputing 77 (1) (2012) 36–47.

[9] M. Lopez-Ramirez, L. Ledesma-Carrillo, E. Cabal-Yepez, C. Rodriguez-Donate, H. Miranda-Vidales, A. Garcia-Perez, EMD-based feature extraction for power quality disturbance classification using moments, Energies 9 (7) (2016) 565.

[10] J. Wang, Z. Xu, Y. Che, Power quality disturbance classification based on compressed sensing and deep convolution neural networks, IEEE Access 7 (2019) 78336–78346.

[11] M. Gok, I. Sefa, Research and implementation of a USB interfaced real-time power quality disturbance classification system, Adv. Electr. Comput. Eng. 17 (3) (2017) 61–70.

[12] A. Enshaee, P. Enshaee, A new S-transform-based method for identification of power quality disturbances, Arab. J. Sci. Eng. 43 (6) (2018) 2817–2832.

[13] F.H.M. Noh, M.A. Rahman, M.F. Yaakub, Performance of modified s-transform for power quality disturbance detection and classification, TELKOMNIKA (Telecommun. Comput. Electr. Control) 15 (4) (2017) 1520–1529.

[14] S. Aziz, M.U. Khan, A. Usman, A. Mobeen, et al., Pattern analysis for classification of power quality disturbances, in: 2020 International Conference on Emerging Trends in Smart Technologies, ICETST, IEEE, 2020, pp. 1–5.

[15] E.G. Ribeiro, T.M. Mendes, G.L. Dias, E.R. Faria, F.M. Viana, B.H. Barbosa, D.D. Ferreira, Real-time system for automatic detection and classification of single and multiple power quality disturbances, Measurement 128 (2018) 276–283.

[16] A. Shaik, A.S. Reddy, Flexible entropy based feature selection and multi class SVM for detection and classification of power quality disturbances, Int. J. Intell. Eng. Syst. 11 (5) (2018).

[17] F. Ucar, O.F. Alcin, B. Dandil, F. Ata, Power quality event detection using a fast extreme learning machine, Energies 11 (1) (2018) 145.

[18] R. Ahila, V. Sadasivam, K. Manimala, An integrated PSO for parameter determination and feature selection of ELM and its application in classification of power system disturbances, Appl. Soft Comput. 32 (2015) 23–37.

[19] I. Parvez, M. Aghili, A.I. Sarwat, S. Rahman, F. Alam, Online power quality disturbance detection by support vector machine in smart meter, J. Mod. Power Syst. Clean Energy 7 (5) (2019) 1328–1339.

[20] N. Ghaffarzadeh, A new method for power quality events detection and classification using discrete wavelet transform and correlation coefficients, Int. J. Ind. Electr. Control Optim. 4 (1) (2021) 47–57.

[21] Y. Shen, M. Abubakar, H. Liu, F. Hussain, Power quality disturbance monitoring and classification based on improved PCA and convolution neural network for wind-grid distribution systems, Energies 12 (7) (2019) 1280.

[22] O.J. Singh, D.P. Winston, B.C. Babu, S. Kalyani, B.P. Kumar, M. Saravanan, S.C. Christabel, Robust detection of real-time power quality disturbances under noisy condition using FTDD features, Automatika: Čas. Autom. Mjer. Elektron. RaČun. Komun. 60 (1) (2019) 11–18.

[23] X. Chen, K. Li, J. Xiao, Classification of power quality disturbances using dual strong tracking filters and rule-based extreme learning machine, Int. Trans. Electr. Energy Syst. 28 (7) (2018) e2560.

[24] J. Wang, Z. Xu, Y. Che, Power quality disturbance classification based on DWT and multilayer perceptron extreme learning machine, Appl. Sci. 9 (11) (2019) 2315.

[25] M.I. Gursoy, A.S. Yilmaz, S.V. Ustun, A practical real-time power quality event monitoring applications using discrete wavelet transform and artificial neural network, J. Eng. Sci. Technol. 13 (6) (2018) 1764–1781.

[26] N. Minh Khoa, L. Van Dai, Detection and classification of power quality disturbances in power system using modified-combination between the stockwell transform and decision tree methods, Energies 13 (14) (2020) 3623.

[27] T. Zhong, S. Zhang, G. Cai, N. Huang, Power-quality disturbance recognition based on time-frequency analysis and decision tree, IET Gener. Transm. Distrib. 12 (18) (2018) 4153–4162.

[28] T. Zhong, S. Zhang, G. Cai, Y. Li, B. Yang, Y. Chen, Power quality disturbance recognition based on multiresolution S-transform and decision tree, IEEE Access 7 (2019) 88380–88392.

[29] F. Zaro, S. Alqam, Power quality detection and classification using S-transform and rule-based decision tree, 2019.

[30] W. Qiu, Q. Tang, J. Liu, Z. Teng, W. Yao, Power quality disturbances recognition using modified s transform and parallel stack sparse auto-encoder, Electr. Power Syst. Res. 174 (2019) 105876.

[31] J. Li, Z. Teng, Q. Tang, J. Song, Detection and classification of power quality disturbances using double resolution S-transform and DAG-svms, IEEE Trans. Instrum. Meas. 65 (10) (2016) 2302–2312.

[32] K. Cai, B.P. Alalibo, W. Cao, Z. Liu, Z. Wang, G. Li, Hybrid approach for detecting and classifying power quality disturbances based on the variational mode decomposition and deep stochastic configuration network, Energies 11 (11) (2018) 3040.

[33] A.A. Abdoos, P.K. Mianaei, M.R. Ghadikolaei, Combined VMD-svm based feature selection method for classification of power quality events, Appl. Soft Comput. 38 (2016) 637–646.

[34] M.R. Alam, F. Bai, R. Yan, T.K. Saha, Classification and visualization of power quality disturbance-events using space vector ellipse in complex plane, IEEE Trans. Power Deliv. 36 (3) (2020) 1380–1389.

[35] M.A. Rodriguez, J.F. Sotomonte, J. Cifuentes, M. Bueno-López, Power quality disturbance classification via deep convolutional auto-encoders and stacked LSTM recurrent neural networks, in: 2020 International Conference on Smart Energy Systems and Technologies, SEST, IEEE, 2020, pp. 1–6.

[36] S. Ekici, F. Ucar, B. Dandil, R. Arghandeh, Power quality event classification using optimized Bayesian convolutional neural networks, Electr. Eng. 103 (1) (2021) 67–77.

[37] IEEE recommended practice for monitoring electric power quality, ieee std 1159-2019 (revision of ieee std 1159-2009), 2019, pp. 1–98, http://dx.doi.org/10.1109/IEEESTD.2019.8796486.

[38] M.U. Khan, S. Aziz, K. Iqtidar, G.F. Zaher, S. Alghamdi, M. Gull, A two-stage classification model integrating feature fusion for coronary artery disease detection and classification, Multimedia Tools Appl. 81 (10) (2022) 13661–13690.

[39] S. Aziz, M.U. Khan, K. Iqtidar, S. Ali, A.N. Remete, M.A. Javid, Pulse plethysmograph signal analysis method for classification of heart diseases using novel local spectral ternary patterns, Expert Syst. (2022) e13011.

[40] M.U. Khan, S. Aziz, K. Iqtidar, R. Fernandez-Rojas, Computer-aided diagnosis system for cardiac disorders using variational mode decomposition and novel cepstral quinary patterns, Biomed. Signal Process. Control 81 (2023) 104509.

[41] S. Aziz, M. Awais, T. Akram, U. Khan, M. Alhussein, K. Aurangzeb, Automatic scene recognition through acoustic classification for behavioral robotics, Electronics 8 (5) (2019) 483.

[42] S. Aziz, M.U. Khan, M. Alhaisoni, T. Akram, M. Altaf, Phonocardiogram signal processing for automatic diagnosis of congenital heart disorders through fusion of temporal and cepstral features, Sensors 20 (13) (2020) 3790.

[43] S. Aziz, M.U. Khan, A. Rehman, Z. Tariq, K. Iqtidar, Computer-aided diagnosis of COVID-19 disease from chest x-ray images integrating deep feature extraction, Expert Syst. 39 (5) (2022) e12919.

[44] M.U. Khan, S. Aziz, A novel pulse plethysmograph signal analysis method for identification of myocardial infarction, dilated cardiomyopathy, and hypertension, Turk. J. Electr. Eng. Comput. Sci. 29 (2) (2021) 962–977.

[45] S. Aziz, M. Awais, M.U. Khan, K. Iqtidar, U. Qamar, Classification of cardiac disorders using 1D local ternary patterns based on pulse plethysmograph signals, Expert Syst. 38 (3) (2021) e12664.

[46] U. Singh, S.N. Singh, A new optimal feature selection scheme for classification of power quality disturbances based on ant colony framework, Appl. Soft Comput. 74 (2019) 216–225.

[47] D. Akmaz, A new signal processing approach/method for classification of power quality disturbances, Digit. Signal Process. 130 (2022) 103701.

[48] M. Lopez-Ramirez, E. Cabal-Yepez, L.M. Ledesma-Carrillo, H. Miranda-Vidales, C. Rodriguez-Donate, R.A. Lizarraga-Morales, FPGA-based online PQD detection and classification through DWT, mathematical morphology and SVD, Energies 11 (4) (2018) 769.

[49] S. Khokhar, A.A.M. Zin, A.P. Memon, A.S. Mokhtar, A new optimal feature selection algorithm for classification of power quality disturbances using discrete wavelet transform and probabilistic neural network, Measurement 95 (2017) 246–259.
[50] B. Panigrahi, V.R. Pandi, Optimal feature selection for classification of power quality disturbances using wavelet packet-based fuzzy k-nearest neighbour algorithm, IET Gener. Transm. Distrib. 3 (3) (2009) 296–306.
[51] A. Usman, M.A. Choudhry, A precision detection technique for power disturbance in electrical system, Electr. Eng. 104 (2) (2022) 781–796.
[52] H. Liu, F. Hussain, Y. Shen, S. Arif, A. Nazir, M. Abubakar, Complex power quality disturbances classification via curvelet transform and deep learning, Electr. Power Syst. Res. 163 (2018) 1–9.
[53] D. Sabin, Recommended practice for power quality data interchange format (PQDIF), 2019, URL https://grouper.ieee.org/groups/1159/3/, urldate= 2022-10-30.
[54] R. Entso-E, Frequency stability evaluation criteria for the synchronous zone of continental europe, 2016.